Control of a Separation Column for ^{18}O Isotope Production

Vlad Mureşan, Mihail Abrudean, Honoriu Vălean, Liviu Miclea, Mihaela-Ligia Ungureşan*, Iulia Clitan, Adela Puşcaşiu, Alexandra Fanca

*Automation Department, *Physics and Chemistry Department*
Technical University of Cluj-Napoca
Cluj-Napoca, Romania
email addresses: Vlad.Muresan@aut.utcluj.ro, Mihail.Abrudean@aut.utcluj.ro, Honoriu.Valean@aut.utcluj.ro, Liviu.Miclea@aut.utcluj.ro, Mihaela.Unguresan@chem.utcluj.ro, Iulia.Inoan@aut.utcluj.ro, Adela.Puscasiu@aut.utcluj.ro, Alexandra.Fanca@aut.utcluj.ro

***Abstract*— In the paper, a method to control the strong nonlinear process associated to a separation column used for the ^{18}O isotope production, is presented. In order to obtain an accurate process model, neural networks are used. The proposed control strategy is analyzed both in the case when the main disturbance signals occur and they do not occur in the system. In order to improve the control system performances, the theory of fractional-order controllers is applied, combined with an adaptive algorithm. For a more efficient disturbances effect rejection, the reference model of the separation process is used.**

Keywords*— separation column; ^{18}O isotope; neural model; PID controller; fractional-order controller; disturbance compensation; distributed parameter process

I. Introduction

Solutions to control an ^{18}O separation process were approached in papers from technical literature, for example [1,2], but they are based on a lumped parameter model of the process. In this paper, the proposed control strategy is implemented based on a distributed parameter model, fact which increases significantly the modeling – control validity. The separation plant (including the separation column and the equipment of the refluxing system) for the ^{18}O isotope is presented in Fig. 1. Using this plant, the ^{18}O isotope separation is made through isotopic exchange in the system NO, NO_2-H_2O, HNO_3 [3,4]. In Fig. 1, FSC is the Final Separation Column, the term "Final" being used due to the fact that this column works as the final column of a separation cascade which contains two separation columns. The main aim of this paper is to control the FSC work in the case when it works independently from the separation cascade. The results of this research activity, consisting from the proposed control strategy, will be further used in order to find an appropriate method to control the separation cascade.The height of FSC is h = 10 m, containing in its structure 5 equal sectors (S1 – S5), and the FSC diameter is d = 14 mm. In order to produce the ^{18}O isotope, the nitric oxides (NO, NO_2) which are introduced in the lower part of the column, are circulated in counter-current with the nitric acid (HNO_3) – solution which is introduced in the upper part of the column. The notation used for the input flow of nitric oxides F_i and the notation used for the output flow of nitric acid is F_W (F_W represents, also, the isotopic waste of the separation process). With F_o, the output flow of the nitric oxides from FSC is notated. The nitric oxides which exit from FSC in its upper part are circulated to the arc-cracking reactor ACR. ACR is used to generate at its output, both nitrogen (N_2) and nitric oxides (NO, NO_2), with an increase in the concentration of NO_2 (the flow of N_2, NO and NO_2 is notated with F_N). The absorption of the nitric oxides in water is made in the absorber A, resulting the nitric acid solution which supplies FSC (the notation used for the flow of nitric acid solution is F_A). The water used to supply the absorber A (having the flow F_{H2O}) is produced using the catalytic reactor CR (in CR, the amount of nitrogen and nitric oxide from the absorber output having the flow F_{NN} (NO, N_2) reacts with with the hydrogen with which CR is supplied (the hydrogen flow at the CR input is F_H). The excess of both nitrogen and hydrogen resulted after the reaction is evacuated from CR under the flow F_{NH}.

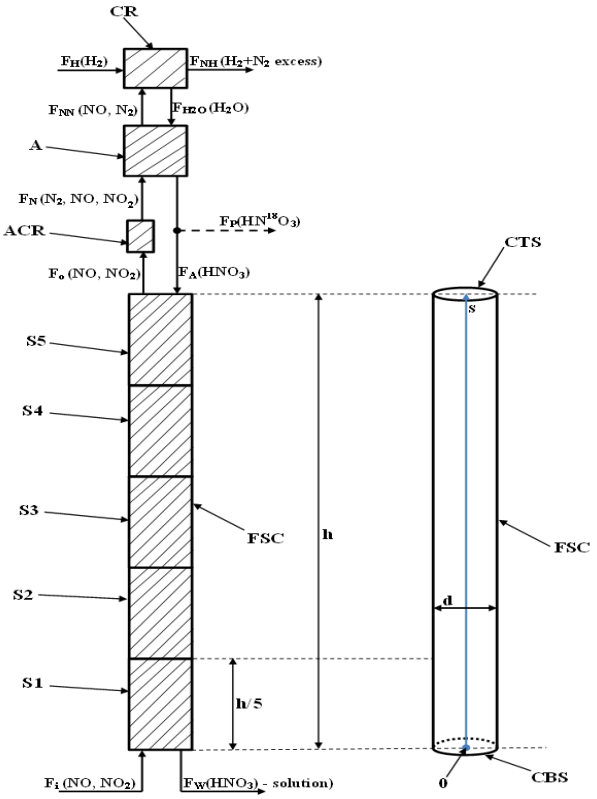

Fig. 1. The separation plant for the ^{18}O isotope (including the separation column and the equipment of the refluxing system)

The product extraction can be made from the FSC top under the form of nitric acid with an increased concentration of ^{18}O isotope ($HN^{18}O_3$). The notation used for the product flow is F_P. The pipe used for extracting the product is figured with dashed line due to the fact that in this approach, only the total reflux ($F_P = 0$) working regime is considered. The elements from the previous figure which are hachured contain packing (steel packing of Heli-Pack type in the case of FSC and in the case of the reactors (ACR and CR)) and ceramic packing in the case of the absorber A.

II. Isotope Exchange Process Modeling

The ^{18}O isotope separation process is a distributed parameter one [5,6], the main output signal (the ^{18}O isotope concentration notated with y(t,s)) depending on two independent variables: time (t) and the position in FSC height (s). For highlighting the position in FSC height, the (0s) axis belonging to a Cartesian system is defined (in Fig. 1). The (0s) axis origin is (0) representing the centre of the Column Base Section (CBS). The independent variable (s) has an increasing evolution from the column base to the column top and its maximum value can be obtained for s = h, corresponding to the Column Top Section (CTS). The main input signal in the process is the input flow of nitric oxides $F_i(t)$. The mathematical model is determined in the hypothesis when FSC works in total reflux regime ($F_P = 0$). This regime is used in the first part of the plant working with the purpose to increase the ^{18}O isotope concentration until the imposed value, at the column top, is reached. This working regime is the most relevant one for determining the FSC dynamics in relation to both independent variables. All the structure parameters of the proposed mathematical model are determined by processing experimental data obtained using the real plant [3,4]. The proposed mathematical model for the separation process work consists in using of an improved form of the approximating function [7] from (1) for describing the evolution of the output signal in relation to the two independent variables:

$$y(t,s) = y_0 + F_T(t) \cdot F_S(s) \quad (1)$$

where the function $F_T(t)$ models the process dynamics in relation to (t), the function $F_S(s)$ models the process dynamics in relation to (s) and $y_0 = 0.204\%$ is the natural abundance of the ^{18}O isotope. Based on the experimental step response of the real separation plant, the conclusion that the process dynamics in relation to (t) is a first order one, resulted. Consequently, in order to obtain the $F_T(t)$ function, the identification of the process time constant T and the mathematical construction of the equivalent input signal which implies the direct variation of the $F_T(t)$ function, are necessary. Using the experimental data, the fact that the process time constant is a function depending on the input signal $F_i(t)$, is concluded and it can be approximated using the equation:

$$T(F_i) = g_1 + \frac{g_2}{F_i} \quad (2)$$

where the two constants have the values $g_1 = -188$ h and $g_2 = 58000$ l. The equivalent input signal has the significance of the ^{18}O concentration increase over y_0, in steady state regime and for s = h, being given by:

$$u_t = y(t_f, s = h) - y_0 = y_0 \cdot (SEP(F_i) - 1) = y_0 \cdot (\alpha^{\frac{h}{HETP(F_i)}} - 1) \quad (3)$$

where (t_f) represents the final value for (t) (highlighting the process settling time). Also, $SEP(F_i) = \alpha^{\frac{h}{HETP(F_i)}}$ is the separation of the column and $HETP(F_i)$ represents the Height of Equivalent Theoretical Plate. Both SEP and HETP functions depend on the input signal $F_i(t)$. Also, $\alpha = 1.018$ represents the elementary separation factor of the ^{18}O isotope for the applied isotopic exchange procedure. The result of the ratio $\frac{h}{HETP(F_i)}$ gives the number of the theoretical plates. The $HETP(F_i)$ has a nonlinear form (linear on intervals, but nonlinear on the entire domain of the input signal values) which is determined from the experimental data, being given by the following system of equations:

$$\begin{cases} HETP(F_i) = HETP_0 + K_{H1} \cdot (F_i - F_0), \text{if } F_i \le 140 l/h \\ HETP(F_i) = HETP_0 + K_{H2} \cdot (F_i - F_0), \text{if } F_i > 140 l/h \end{cases} \quad (4)$$

In (4) $HETP_0 = 8.6$ cm is the minimum value of $HETP(F_i)$ function obtained for the input flow $F_0 = 140$ l/h, and K_{H1}, respectively K_{H2} ($K_{H1} = -0.08 \frac{cm \cdot h}{l}$ for $F_i \le 140$ l/h ; $K_{H2} = 0.0333 \frac{cm \cdot h}{l}$ for $F_i > 140$ l/h) are the gradients of the two ramps from (4). Using (2) and (3), the $F_T(t)$ function represents the solution of the following ordinary differential equation:

$$\frac{dF_T(t)}{dt} = -\frac{1}{T(F_i)} \cdot F_T(t) + \frac{1}{T(F_i)} \cdot u_t \quad (5)$$

The differential equation from (5) is solved only after the value of the T time constant is singularized for a certain (F_i). The $F_s(s)$ function models the concentration evolution on the column height, being given by:

$$F_s(s) = \frac{e^{\frac{s}{S}} - 1}{e^{\frac{s_f}{S}} - 1} \quad (6)$$

where $S(F_i)$ represents the "height" constant of the separation column. S depends on $F_i(t)$ due to the HETP variation in relation to $F_i(t)$. Practically, (6) generates the proportion of the ^{18}O isotope concentration in a certain position from the FSC height, in relation to the ^{18}O isotope concentration at the FSC top, for a certain value of $F_i(t)$. The $S(F_i)$ function is experimentally determined being given by the system of two equations :

$$\begin{cases} S(F_i) = S_1 + K_{S1} \cdot (F_i - F_1), \text{if } F_i \le 140 l/h \\ S(F_i) = S_2 + K_{S2} \cdot (F_i - F_2), \text{if } F_i > 140 l/h \end{cases} \quad (7)$$

where $S_1 = 751.124$ cm is obtained for $F_1 = 80$ l/h and $S_2 = 565.5$ cm is obtained for $F_2 = 185$ l/h. Also, K_{S1} and K_{S2} ($K_{S1} = -4.4804 \frac{cm \cdot h}{l}$ for $F_i \le 140$ l/h ; $K_{S2} = 1.8489 \frac{cm \cdot h}{l}$ for $F_i > 140$ l/h) are the gradients of the two ramps from (7). As in the case of $HETP(F_i)$ function, $S(F_i)$ has an evolution

linear on intervals, but nonlinear on the entire domain of the input signal values.

Due to their nonlinearity, the behavior of the $u_t(F_i)$, $T(F_i)$ and $S(F_i)$ functions is learned simultaneously using a feed-forward fully connected neural network [8,9] which has the structure presented in Fig. 2. The proposed neural network has one input signal $m = F_i$ and three output signals $y_{o1} = u_t(F_i)$, $y_{o2} = T(F_i)$, respectively $y_{o3} = S(F_i)$. Also, it contains $n = 29$ neurons in the hidden layer, having as activation function the hyperbolic tangent and three linear neurons in the output layer. The proposed neural network is trained using the Levenberg–Marquardt algorithm applied on 1050 input-output samples and imposing the maximum limit of 20000 training epochs. The training solution is obtained after the run of all 20000 epochs. In order to test the accuracy of the obtained solution, we have used as quality indicator the Mean Square Error (MSE). After the computation of MSE between the experimental values of the three functions and the values resulted by the simulation of the trained neural network, using 1050 samples, we obtain $MSE1 = 1.851 \cdot 10^{-4}$ % for y_{o1}, $MSE2 = 1.278 \cdot 10^{-4}$ h for y_{o2} and $MSE3 = 5.7 \cdot 10^{-3}$ m for y_{o3}. These values of MSE which are practically insignificant in comparison with the usual values of the three signals prove the high quality of the approximation of the separation process structure parameters.

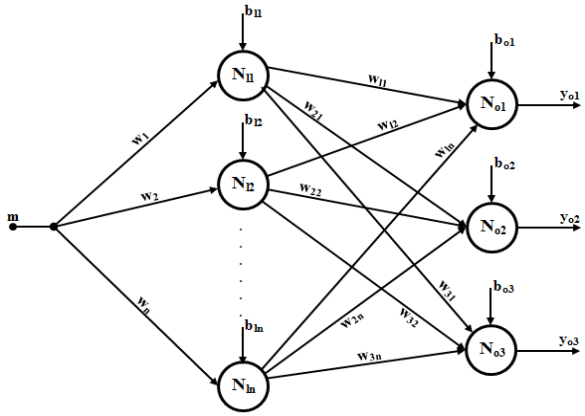

Fig. 2. The structure of the proposed neural network used for learning the $u_t(F_i)$, $T(F_i)$ and $S(F_i)$ functions

The structure parameters of the separation process can be obtained by applying the following equation:

$$Y_0(m) = W_2 \cdot \tanh(m \cdot W_1 + B_1) + B_2 \qquad (8)$$

where $Y_0(m)^T = [y_{01}\ y_{02}\ y_{03}]$ is the output vector presented in transposed form (fact highlighted by the notation "*T*"), the vector $W_1(n\times1)$ contains the training solutions obtained for the input weights w_i ($i \in \{1, 2,..., n\}$), the vector B_1 contains the training solutions obtained for the bias values of the neurons from the hidden layer b_{1i} ($i \in \{1, 2,..., n\}$), the matrix $W_2(3\times n)$ contains the training solutions obtained for the weights which connect the hidden layer with the output layer w_{ji} ($j \in \{1, 2, 3\}$, $i \in \{1, 2,..., n\}$) and the vector $B_2(3\times1)$ contains the training solutions obtained for the bias values of the neurons from the output layer b_{oj} ($j \in \{1, 2, 3\}$). Also, the notation "tanh" signifies the hyperbolic tangent function.

III. The Proposed Control Strategy and the Controllers Tuning

The proposed control structure which can be used with high performances for the control of the ^{18}O isotope concentration is presented in Fig. 3. The IEDPP (Isotope Exchange Distributed Parameter Process) represents the controlled separation process, the input signal in it being $F_t(t)$ (the total input flow of nitric oxides) and the output signal from it being the concentration y(t,s) (the second independent variable (s) is introduced as an input signal).

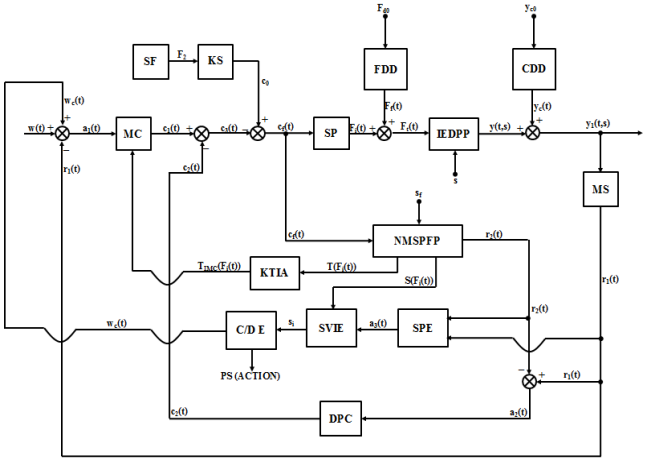

Fig. 3. The proposed control structure

The element NMSPFP represents the Neural Model of the Separation Process Fixed Part which include the neural model of the actuator (SP – Supplying Pump with nitric oxides), the model of IEDPP (presented in the previous Section) and the neural model of the concentration sensor (MS – mass spectrometer). Both SP and MS are linear first order elements and for the learning of the behavior of each, two ARX (Autoregressive with Exogenous Inputs) neural structures, having 12 linear neurons in the hidden layer and one linear neuron in the output layer are used. Also the two ARX neural structures contain each a unit delay on the input signal and a unit delay on the output signal (due to the fact that the two elements are of first order). The IEDPP model is implemented using the solution neural network presented in Fig. 2 which generates the three process structure parameters. Using the first two structure parameters, (5) can be implemented based on the usage of a numerical integrator and using the third one, (6) can be implemented, too. Having (5) and (6), (1) results directly. The automation equipment used in the structure from Fig. 3 work using unified current signals (4-20) mA. The Main Controller (MC) is of PID (Proportional – Integral – Derivative) type [8,9], its feedback signal $r_1(t)$ being generated by the MS. In order to improve the control system performances, the initial form of MC is modified into an adaptive form. In this context, the $T(F_i(t))$ function generated through the run of NMSPFP (on a processor or on a process computer) is adapted using KTIA (Integral Time Constant Adapter) element, which generates the integral time constant of MC ($T_{IMC}(F_i(t))$. Obviously, at the change of $F_i(t)$, the T process time constant presents variations and implicitly, as a consequence, the T_{IMC} integral

time constant of the controller will be adapted. For a more efficient rejection of the effect of the two main disturbances ($F_f(t)$ which represents the variations of the input flow of nitric oxides due to the multiple problems which can interfere in SP work and $y_c(t)$ which represents the ^{18}O isotope concentration variation due to the product extraction (even the product extraction is a usefully procedure, it implies the decrease of the ^{18}O isotope concentration in the column, fact which can be interpreted as a disturbance) the DPC (Disturbance Propagation Compensator) is used. DPC processes the $a_2(t)$ error signal obtained similar as in the case of IMC (Internal Model Control) type control structures, representing a measure of all disturbances which occur in the system work (both of $F_f(t)$ and $y_c(t)$, but also of the parametric disturbances). As effect of DPC, the correction signal $c_2(t)$ is generated. The FDD (Flow Disturbance Delay) and CDD (Concentration Disturbance Delay) elements model the two disturbances propagation dynamics into the system (F_{d0} and y_{c0} represent the steady state values of the two disturbances). The final unified current control signal will be $c_f(t) = c_0 - c_1(t) + c_2(t)$ where c_0 represent the corresponding unified current value for the Starting (Initial) Flow (SF) for the input signal, considered in this case F_2 = 185 l/h (KS represents an proportionality constant used to adapt the value of F_2 signal to c_0). As result of the final control effect (due to $c_f(t)$) the SP generates the actuating signal $F_i(t)$. The Signal Processing Element (SPE) has the purpose to extract the components associated to the ^{18}O isotope natural abundance from the values of the unified current feedback signals $r_1(t)$ and $r_2(t)$ and after this procedure to divide them. At the output of SPE, the error signal $a_3(t)$ results which represents a measure of the variation of the (s) independent variable both due to the change of the position of the concentration sensor in relation to the column height and due to all types of disturbances effects (practically the effect of all types of disturbances are equated with variations of (s)). This aspect is possible due to the fact that NMSPFP is always simulated for the reference value $s = s_f$. Processing the input signals $S(F_i(t))$ generated by NMSPFP and $a_3(t)$ generated by SPE, the "s" Variable Identification Element (SVIE) implements (9) and generates the instantaneous value s_1 of the (s) independent variable.

$$s_1 = S(F_i(t)) \cdot \ln[a_3(t) \cdot e^{\frac{s_f}{S(F_i(t))}} + (1 - a_3(t))] \qquad (9)$$

According to the equivalent instantaneous value s_1, The Correction/Decision Element (C/D E) interprets the physical possibility of separation plant work. Consequently, at the reaching of some limit values for s_1, the correction signal $w_c(t)$ for the setpoint is generated. Its effect will be the decrease of the setpoint signal in order to obtain again the physical possibility of using the column (in order to adapt the setpoint signal to the maximum control effort that can be generated). Also, at a minimum limit for s_1, due to disturbances effects or due to the inappropriate change of the concentration sensor position in the column height, the imposed working regime cannot physically be obtained (due to the limitations regarding the control effort) and as an "Action" C/D E can decide the plant stop (PS). As a general remark, in Fig. 3 the notation "w" is used for the setpoint signals, the notation "r" is used for the feedback signals, the notation "c" is used for the control signals, the notation "F" is used for the flows and the notation "y" is used for the ^{18}O isotope concentrations.

The tuning of the MC is made without considering the disturbances in the system (F_{d0} = 0 l/h and y_{c0} = 0%) and without considering the effects of DPC ($c_2(t)$ = 0 mA), of C/D E ($w_c(t)$ = 0 mA) and of KTIA (not considering the connection between KTIA and MC). Having a strong nonlinear process, the MC tuning is made applying the relay method. After applying the method, the Ziegler-Nichols equations for the relay procedure and after fine adjustment of the obtained controller parameters for obtaining better performances, the following form (transfer function) of the initial PID controller (with first order filter) is obtained:

$$H_{PID}(s) = \frac{a \cdot s^2 + c \cdot s + d}{e \cdot s^2 + f \cdot s} \qquad (10)$$

where $a = K_C \cdot T_I \cdot (T_D + T_F) = 1592$ h^2, $c = K_C \cdot (T_I + T_F) = 70.794$ h, $d = K_C = 0.358$, $e = T_I \cdot T_F = 123.214$ h^2 and $f = T_I = 197.143$ h. In the previous equations of the controller coefficients, K_C represents the proportionality constant of the controller, T_I represents the integral time constant of the controller, T_D represents the derivative time constant of the controller and T_F represents the time constant of the first order filter used in order to obtain the feasible form of the controller. In order to improve the performances of the control system, the adaptive form of MC is used, form obtained making the connection between KTIA element and it. The mathematical model of KTIA can be expressed through the usage of a proportionality constant (K_{TIA}):

$$H_{KTIA}(s) = K_{TIA} \qquad (11)$$

In this case the PID controller has the same form as in (10), but in its coefficients equations, it is made the change: $T_I = T_{IMC}(F_i(t))$. The KTIA controller tuning procedure follows the stages: 1. K_{TIA} is initialized with the value 1; 2. the value of K_{TIA} is decreased with $\Delta K_{TIA} = 0.01$ and the simulation of the control system at step type setpoint is repeated; 3. stage 2 is repeated until the response overshoot reaches the maximum allowed limit σ = 1 %; 4. the tuning problem solution is considered the last value of K_{TIA} for which the limit overshoot is not reached. After applying this procedure, the value K_{TIA} = 0.9 is obtained. Another important problem that is necessary to be solved is to avoid the saturation of the actuating signal. Using the adaptive form of MC, the actuating signal presents a variation which is not included between the saturation limits. In this context, a solution to force the variation of the actuating signal between the saturation limit and to improve simultaneously the response settling time is based on the usage of an modified form of MC based on the usage of the fractional--order systems theory [12-14]:

$$H_{PID}(s) = \frac{a \cdot s^2 + b \cdot s^{1+\alpha} + c \cdot s + d}{e \cdot s^2 + f \cdot s} \qquad (12)$$

where $\alpha \in (0,1)$. In (12), the coefficients c, d, e and f have the same equations and values as in the case of (10). The coefficient a is given by $a = K_C \cdot T_I \cdot T_F = 44.107\ h^2$, and coefficient b is given by $b = K_C \cdot T_I \cdot T_D = 1547.9\ h^2$. The value of the ($\alpha$) parameter is determined iteratively following a procedure similar as in the case of K_{TIA} tuning (in this case the α value is decreased at each step with $\Delta\alpha = 0.01$), but having as algorithm stop condition the obtaining of the highest value of (α) for each the actuating signal is enclosed into the saturation limits. After applying the tuning procedure, the value $\alpha = 0.8$ is obtained. The simulation of the fractional-order controller from (12) is based on using a fractional order integrator with the order $(1 - \alpha)$ and on its approximation using a fifth order the Oustoloup filter. It can be remarked that for the efficiently rejecting of the two disturbances effect, the same compensator DPC is obtained. The proposed transfer function for DPC is of PD type with first order filter:

$$H_{DPC}(s) = K_{DPC} \frac{T_{DPC} \cdot s + 1}{T_{f2} \cdot s + 1} \qquad (13)$$

where K_{DPC} is the proportionality constant of DPC, T_{DPC} is its derivative time constant and T_{f2} is the time constant of the first order filter used to obtain the DPC feasible form. The tuning of DPC is made by fixing the values of its time constant at $T_{DPC} = 17$ h and $T_{f2} = 1$ h, respectively by adjusting the value of K_{DPC} imposing the constrain that for the maximum variation of each disturbance signal, in transitory regime, the actuating signal to remain enclosed between the saturation limits. After applying the tuning procedure, the value $K_{DPC} = 0.714$ is obtained.

IV. Simulations Results

All the simulations are made in MATLAB. In Fig. 4, the control system step responses are comparatively presented both in the case of usage the simple PID controller (presented in (10)) and in the case of using the FOPID (adaptive Fractional – Order PID) controller (presented in (11) and considering the control effect of KTIA), if the setpoint concentration is imposed to the value of 1.5 %,

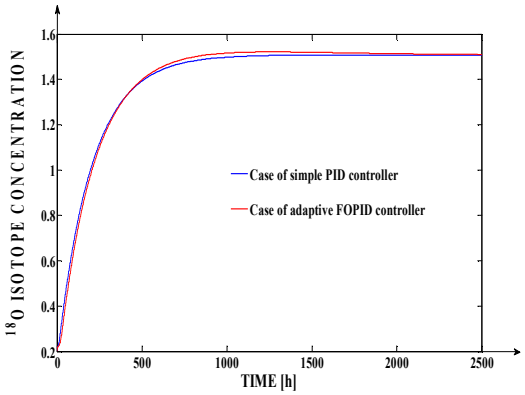

Fig. 4. The step responses of the control system for the cases of using the simple PID controller and of using the adaptive FOPID controller

From Fig. 4, the fact that in steady state regime the two responses reach the imposed values (1.5 %) it results. Consequently, in both cases, the steady state errors are equal to 0% ($e_{st} = 0\%$), the main control purpose being achieved. Also, in both cases the strong constrain that the overshoot value not to increase over 1 % is satisfied. In the case of using the adaptive FOPID controller, we have obtained exactly the overshoot $\sigma_1 = 1$ % (higher than in the case of using the PID controller – $\sigma_2 = 0.4$ %). In this context, in order to analyze which controller generates better controller performances, we have to compare the two responses settling times (the appropriate steady state band near the steady state value of the output signal for this application is considered ±1 %). The two settling times can be determined from Fig.5 in which the same simulation as in the case of Fig. 4 is made but highlighting the responses entering into the steady state band (due to the fact that the two overshoots do not increase over 1 %, the two responses remain enclosed into the band until the next transitory regime occurs).

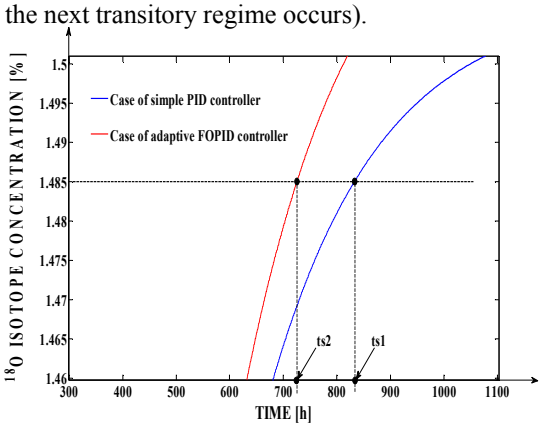

Fig. 5. The settling times associated to the two curves from Fig. 4

From Fig. 5, it results that the settling time obtained in the case of using the adaptive FOPID controller $t_{s2} = 721$ h is significantly lower than the settling time $t_{s1} = 833$ h obtained in the case of using the simple PID controller. The fact that the separation column enters in steady state regime with 112 h faster in the case of using the adaptive FOPID controller than in the case of using the simple PID controller allows the much faster product extraction, aspect which implies a major technological advantage. Consequently, the implementation of the adaptive FOPID controller (it being much more complex than the implementation of simple PID controller) is justified. In Fig. 6, the step responses of the control system (imposing the same setpoint concentration), in the case of using the DPC and the FOPID controller, respectively in the case of using only the simple PID controller, in the context when the two exogenous disturbance signals occur in the system. The disturbance which change directly the value of y(t,s) signal with the steady state value of $y_{c0} = -0.07$ % occur in the system at the moment $t_1 = 2500$ h from the simulation start. From Fig. 6, it results that the effect of this type of disturbance is rejected in both cases, but in the case of using the DPC, the disturbance effect is rejected much faster (after 280 h from t_1; in the case of simple PID controller the disturbance effect is rejected only after 770 h from t_1). In order to highlight the much better performances obtained when the DPC is used, the exogenous disturbance which modifies directly the value of the actuating signal, having the steady state value $F_{d0} = 10$ l/h occur in the system with 500 h earlier (at the moment $t_2 = 4500$ h) in the case of using the simple PID controller. From Fig. 6, it can be

remarked that even in this hypothesis, the effect of the disturbance is rejected faster with 150 h, in the case of using DPC. These aspects prove the efficiency of using the DPC.

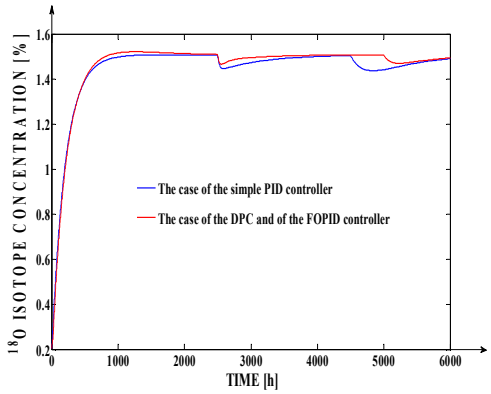

Fig. 6. The step responses of the control structure, in the case when the disturbance signals occur

In Fig, 7, the variation of the s_1 identified variable generated by SVIE is presented.

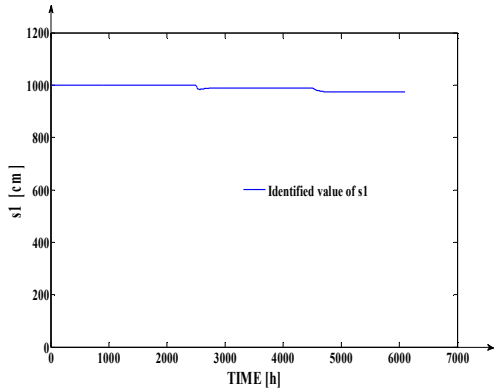

Fig. 7. The variation of the s_1 variable

From Fig. 7, it can be remarked the decrease of s_1 variable after the moments when the two disturbance signals occur in the system.

V. CONCLUSIONS

The paper presents an original solution for modeling and control a strong nonlinear distributed parameter isotopic separation process. The usage of the NMSPFP (Neural Model of the Separation Process Fixed Part) allows the fixed part simulation, without using other elements (for example transducers) and open the possibility to apply both the adaptive control and the disturbances effect compensation. Also, based on NMSPFP (which includes both the neural models of SP and MS, respectively the neural model – proposed in section II – of IEDPP) , a solution to equate the effect of all disturbances which occur in the system with the variation of the (s) independent variable is proposed. The mentioned solution has as applications the possibilities to adapt the setpoint signal in order to maintain the separation column in working regime and, when it is necessary, to stop the separation plant work. The implementation of the advanced control structure presented in Fig. 3 is justified due to the fact that it generates much better performances than a simple negative feedback structure, both in starting regime and in disturbances rejecting regimes. Also, the usage of the adaptive FOPID controller implies the main advantage of obtaining a significantly smaller value of the settling time in comparison with the case of usage a simple PID controller. The proposed model, being a distributed parameter one, can be simulated at the variation of the (s) independent variable, too. The MC is firstly tuned applying a specific method for nonlinear processes, procedure which generates appropriate control performances. The adaption of the controller parameters in relation to the process operating point would be an interesting alternative to the proposed solution but a more laborious one (this new solution would imply the identification of the controller parameters dynamics (dependency) in relation to process operating point). As it was previously mentioned, the usage of the FOPID controller is justified through the consistent improvement of the control system settling time, in the same time the important constrain of obtaining an overshoot value smaller or equal to 1% being respected. The SPE element makes the scaled ratio between the $r_1(t)$ and $r_2(t)$ signals, respectively the mathematical model of SVIE is presented in (9).

REFERENCES

[1] I. Clitan, V. Mureşan, T. Coloşi and M.-L. Ungureşan, "Control structure design for an 18O isotope separation column", Proceedings of AQTR Conference, 19-21 May 2016, pp. 1 – 6.

[2] Pier A. de Groot (editor), Handbook of Stable Isotope Analytical Techniques, Volume II, Elsevier Publishing House, 2009.

[3] D. Axente, M. Abrudean and A. Bâldea, 15N, 18O, 10B, 13C Isotopes Separation trough Isotopic Exchange, Science Book House, 1994.

[4] M. Abrudean, *Ph.D. Thesis*. 1981.

[5] H.-X. Li and C. Qi, Spatio-Temporal Modeling of Nonlinear Distributed Parameter Systems: A Time/Space Separation Based Approach, 1st Edition, Edited by Springer Publishing House, 2011.

[6] A. Smyshlyaev and M. Krstic, "Control design for PDEs with space-dependent diffusivity and time-dependent reactivity," In Automatica, Vol. 41, pp. 1601-1608.

[7] V. Mureşan, M. Abrudean, M.-L. Ungureşan, T. Coloşi, "Modeling and Simulation of the Isotopic Exchange for ^{18}O Isotope Production," Proceedings of AQTR Conference, Cluj-Napoca, 2018.

[8] S. Haykin, Neural Networks and Learning Machines, Third Edition, Edited by Pearson International Edition, 2009, 934 pages.

[9] H. Valean, "Neural Network for System Identification and Modelling," AQTR-1996, Cluj-Napoca, Romania, pp. 263-268, 23-24 May, 1996.

[10] J. Love, Process Automation Handbook, 1 edition, Springer Publishing House, 2007, 1200 pages.

[11] F. Golnaraghi and B. C. Kuo, Automatic Control Systems, 9th edition, edited by Wiley Publishing House, 2009, 800 pages.

[12] C. A. Monje Micharet, Design Methods of Fractional Order Controllers for Industrial Applications, Ph.D. thesis, University of Extremadura, Spain, 2006.

[13] C. A. Monje, Y. Q. Chen, Blas M. Vinagre, D. Xue and V. Feliu, Fractional-order Systems and Controls, Springer Publishing House, 2010, 415 pages.

[14] A. Oustaloup, "From fractality to non integer derivation through recursivity, a property common to these two concepts: a fundamental idea from a new control strategy," 12th IMACS World Congress, Paris, 1998, pp. 203-208.